Supporting Information

Efficient Synthesis and Excellent Antimicrobial Activity of Star-Shaped Cationic Polypeptides with Improved Biocompatibility

Hao Liu,[a] Xu Zhang,[b] Ziyin Zhao,[a] Fangping Yang,[a] Ruizhong Xue,[a] Lichen Yin,[a] Ziyuan Song,[a] Jianjun Cheng,[c] Shifang Luan,[b,*] Haoyu Tang,[a,*]

[a] *Institute of Functional Nano & Soft Materials (FUNSOM), Collaborative Innovation Center of Suzhou Nano Science & Technology, Soochow University, Suzhou 215123, China*

[b] *State Key Laboratory of Polymer Physics and Chemistry, Changchun Institute of Applied Chemistry, Chinese Academy of Sciences, Changchun, 130022, China*

[c] *Department of Materials Science and Engineering, University of Illinois at Urbana−Champaign, Urbana, Illinois 61801, United States*

Correspondence to: Haoyu Tang (Email: hytang@suda.edu.cn) or Shifang Luan (sfluan@ciac.ac.cn)

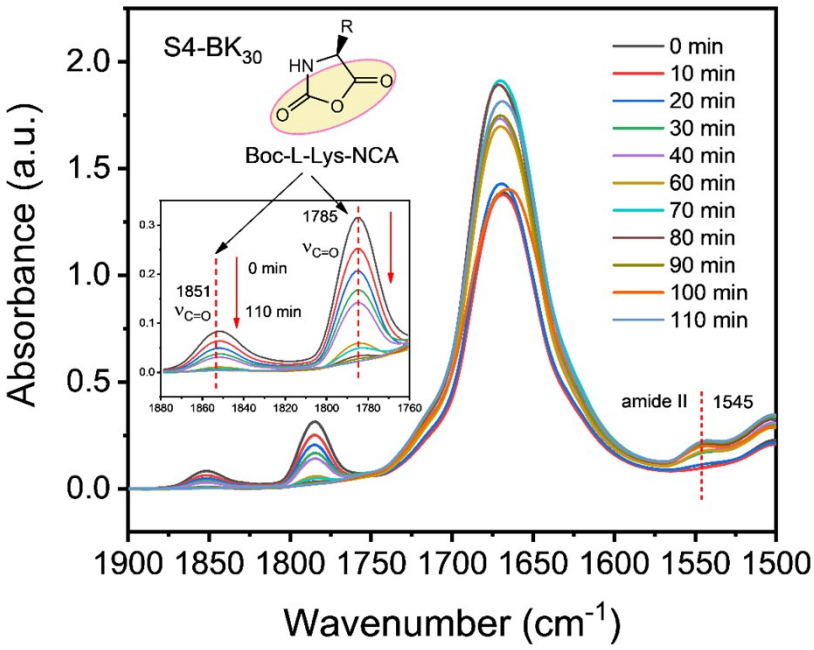

Figure S1. Polymerization process of Boc-$_L$-Lys-NCA initiated by G0-PAMAM in a mixed solvent of DCM and DMF (v/v = 2.5) as measured by FTIR. Polymerization condition: $[M]_0$ = 0.4 M.

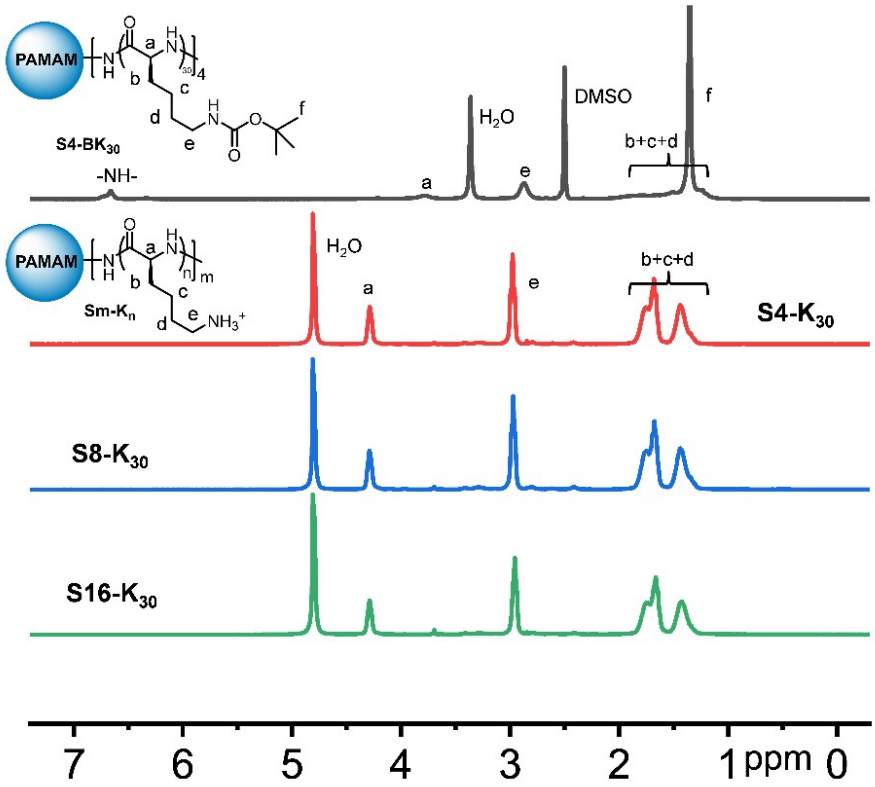

Figure S2. ^{1}H NMR spectra of S4-BK$_{30}$ in DMSO-d$_6$ and S$_m$-K$_n$ (m = 4, 8, 16, n = 30) in D$_2$O.

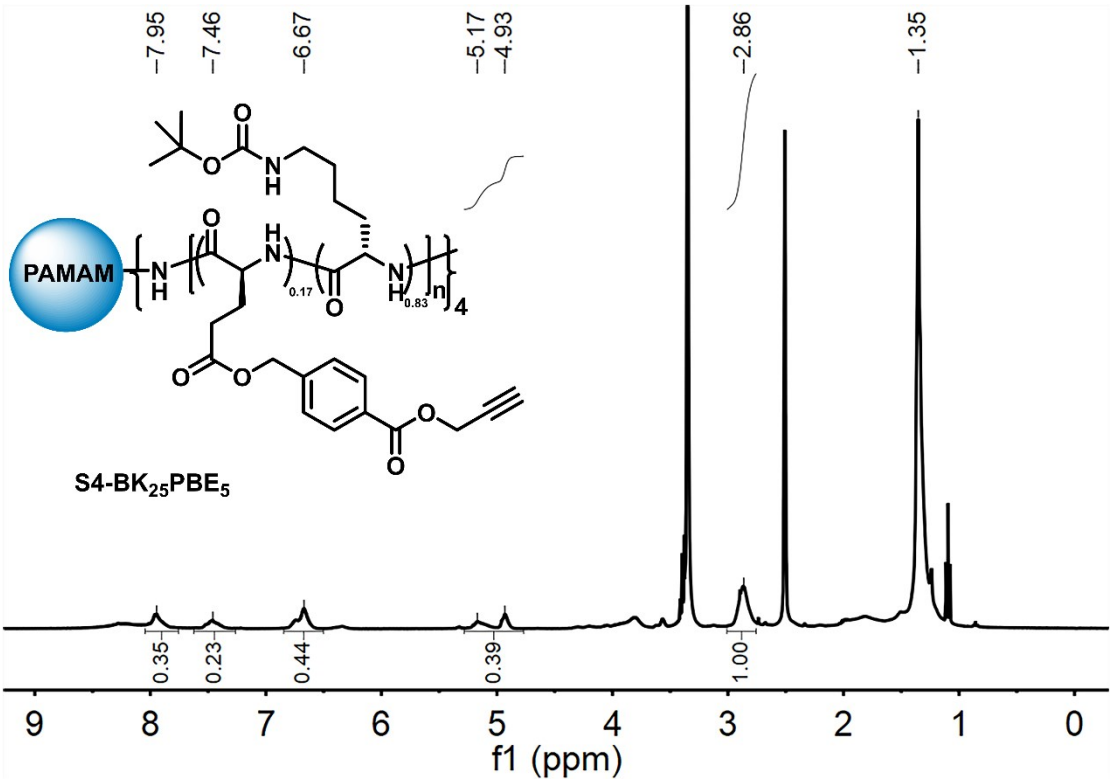

Figure S3. ^{1}H NMR spectrum of S4-$BK_{25}PBE_5$ in DMSO-d_6.

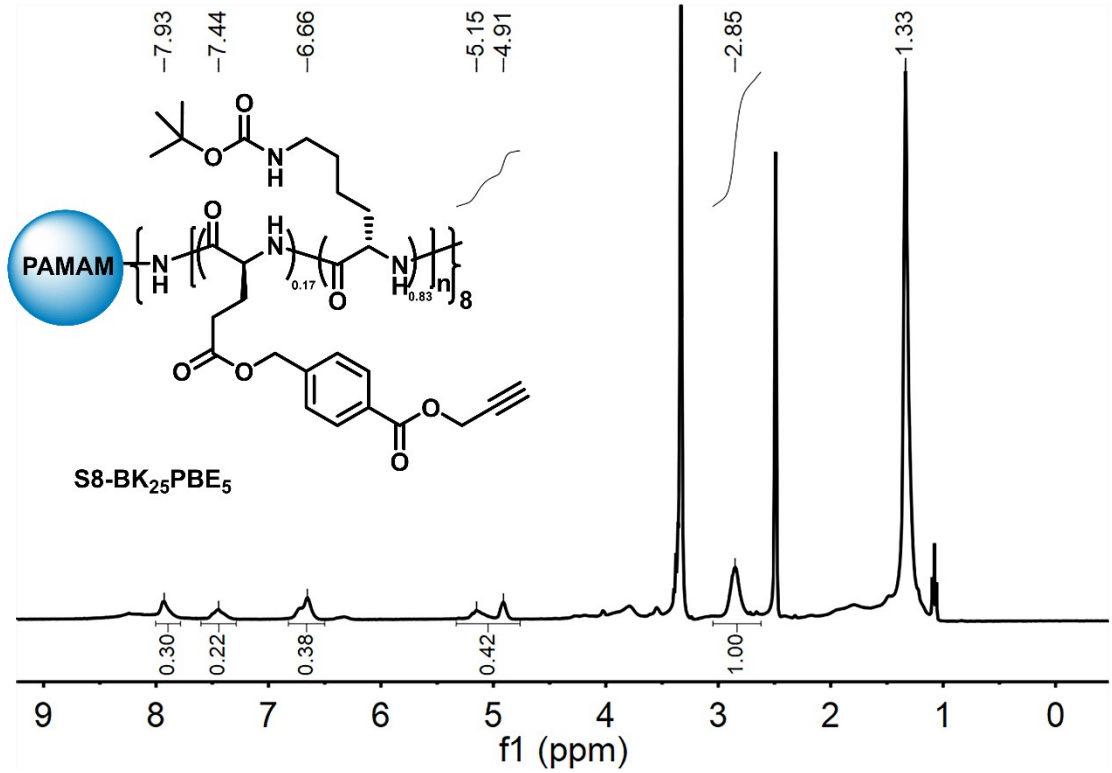

Figure S4. ^{1}H NMR spectrum of S8-$BK_{25}PBE_5$ in DMSO-d_6.

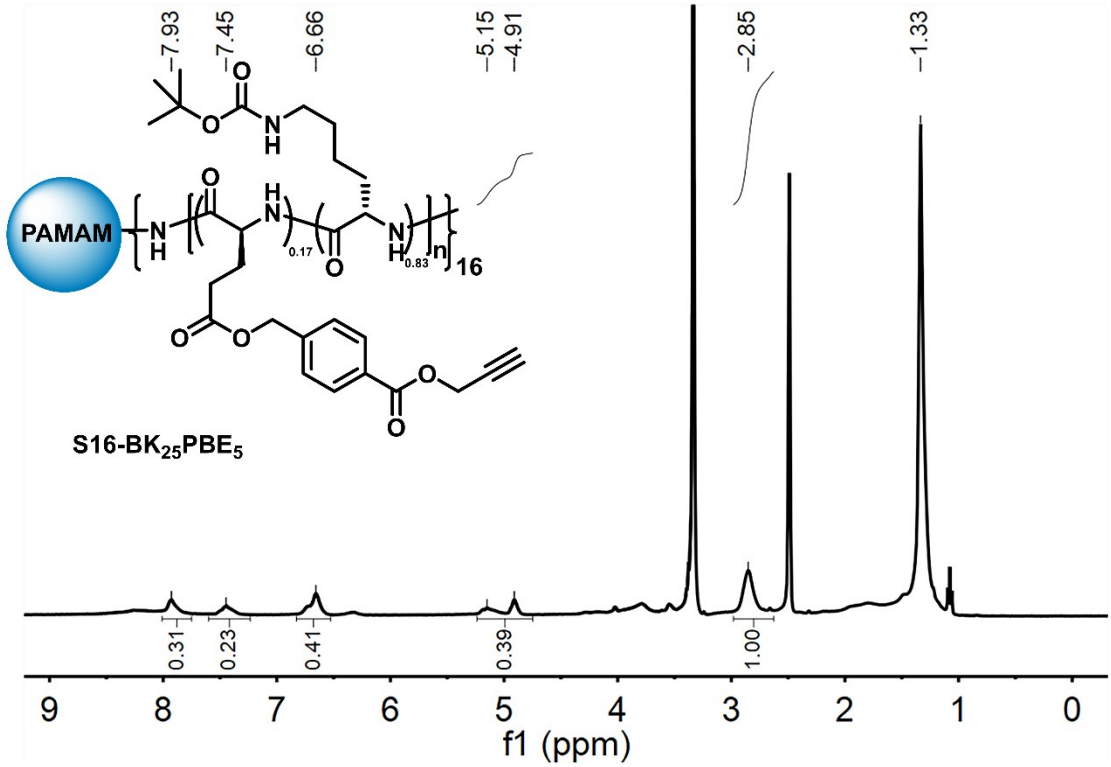

Figure S5. ^{1}H NMR spectrum of S16-$BK_{25}PBE_5$ in DMSO-d_6.

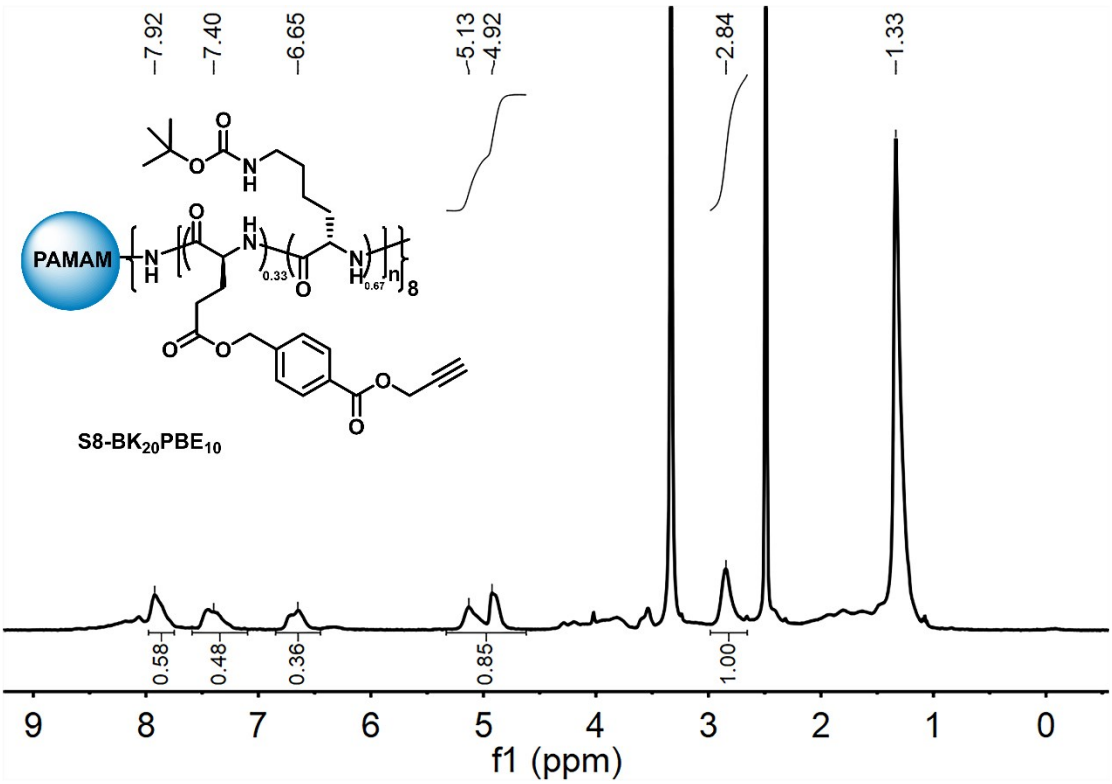

Figure S6. ^{1}H NMR spectrum of S8-$BK_{20}PBE_{10}$ in DMSO-d_6.

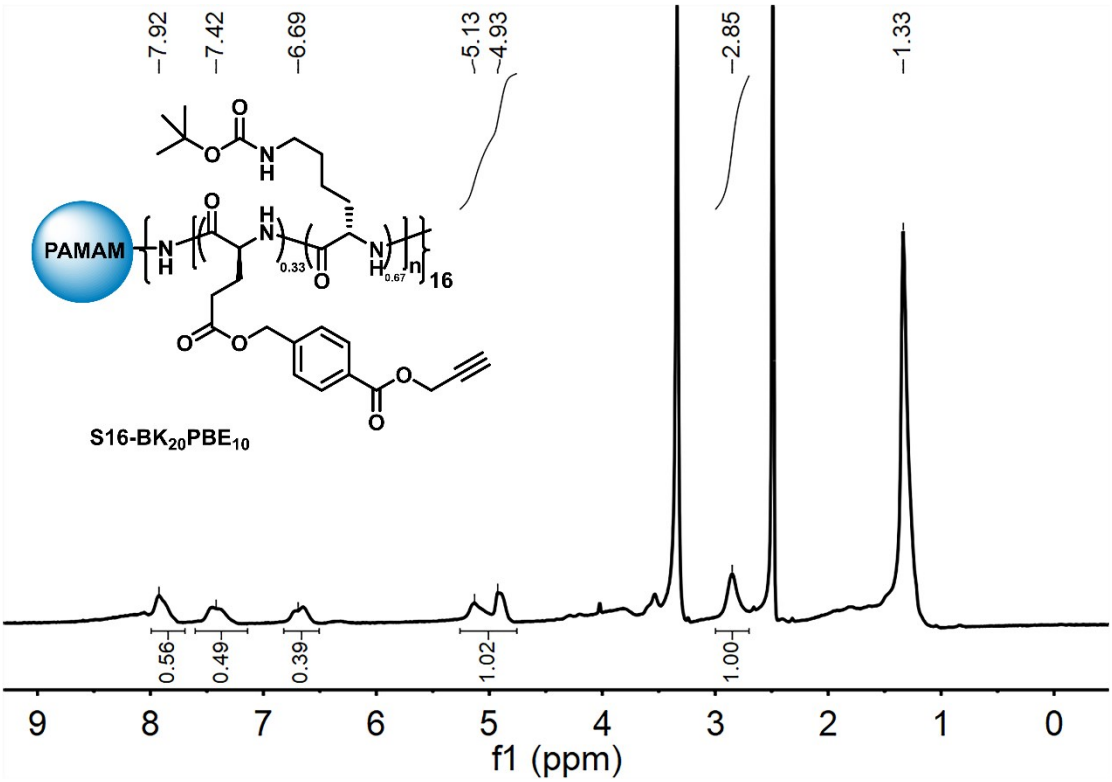

Figure S7. ^{1}H NMR spectrum of S16-$BK_{20}PBE_{10}$ in DMSO-d_6.

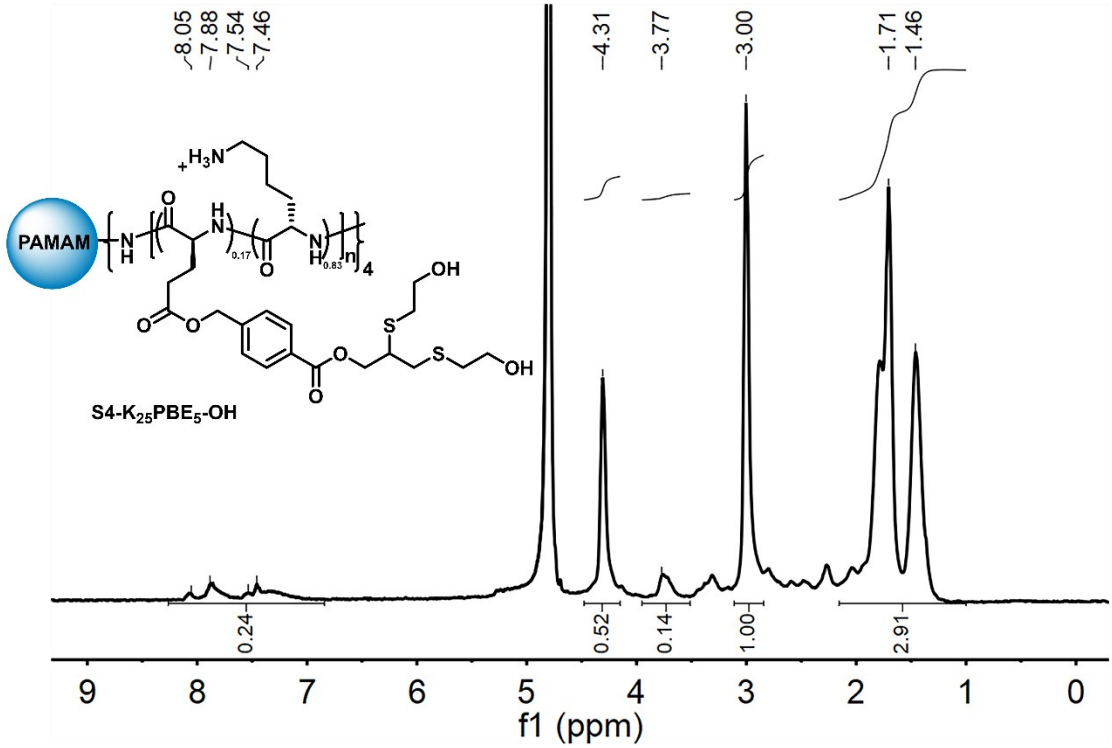

Figure S8. ^{1}H NMR spectrum of S4-$K_{25}PBE_5$-OH in D_2O.

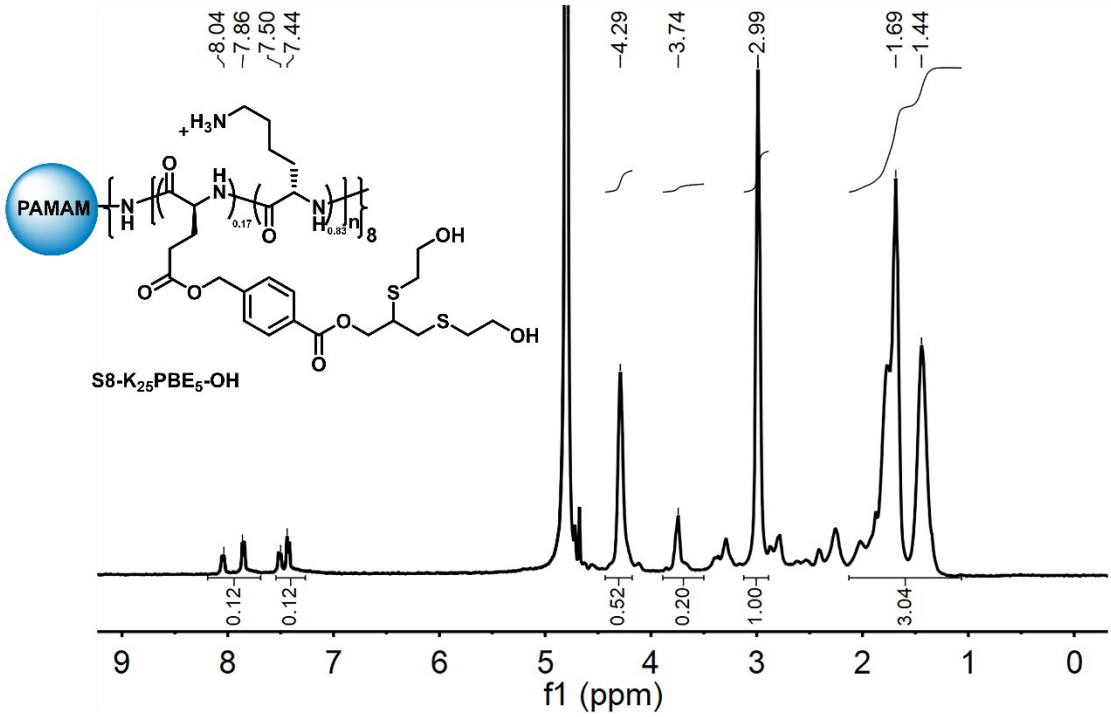

Figure S9. ^{1}H NMR spectrum of S8-$K_{25}PBE_5$-OH in D_2O.

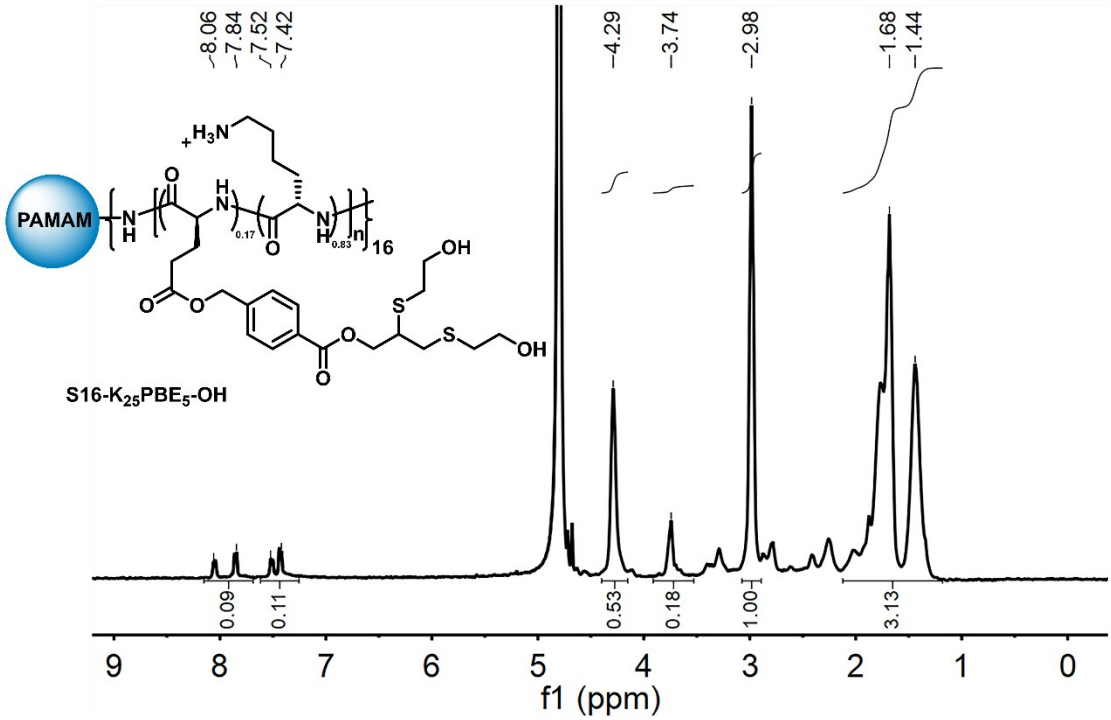

Figure S10. ^{1}H NMR spectrum of S16-$K_{25}PBE_5$-OH in D_2O.

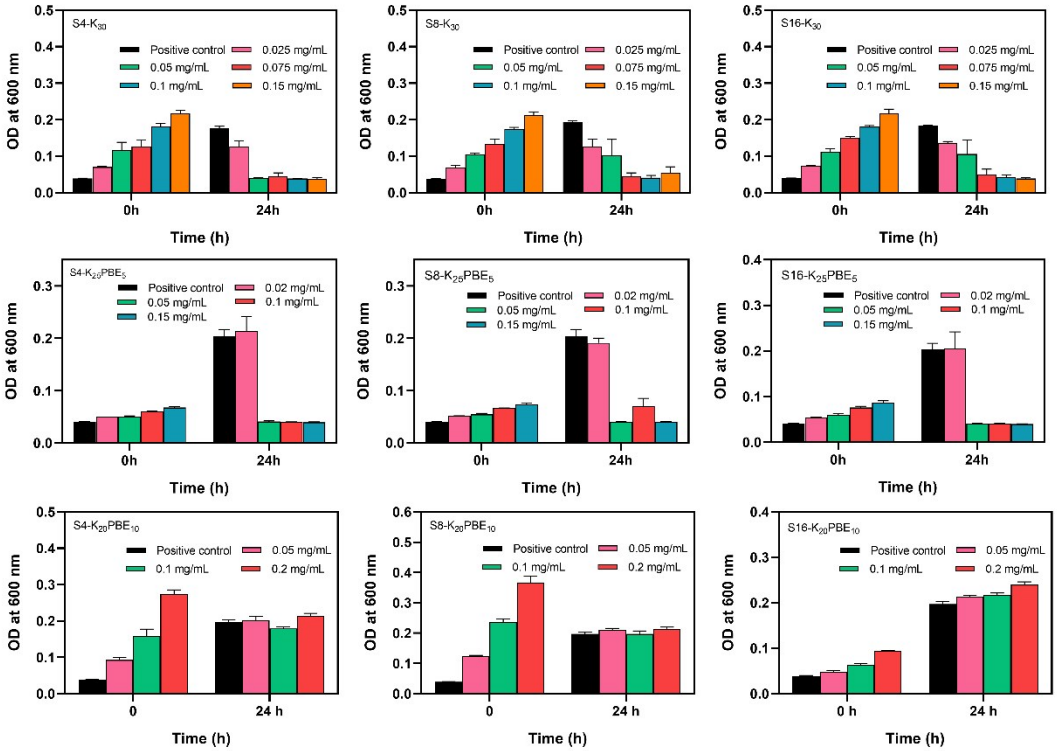

Figure S11. Dose-dependent growth inhibition of *S.aureus* in the presence of the resulting polymers.

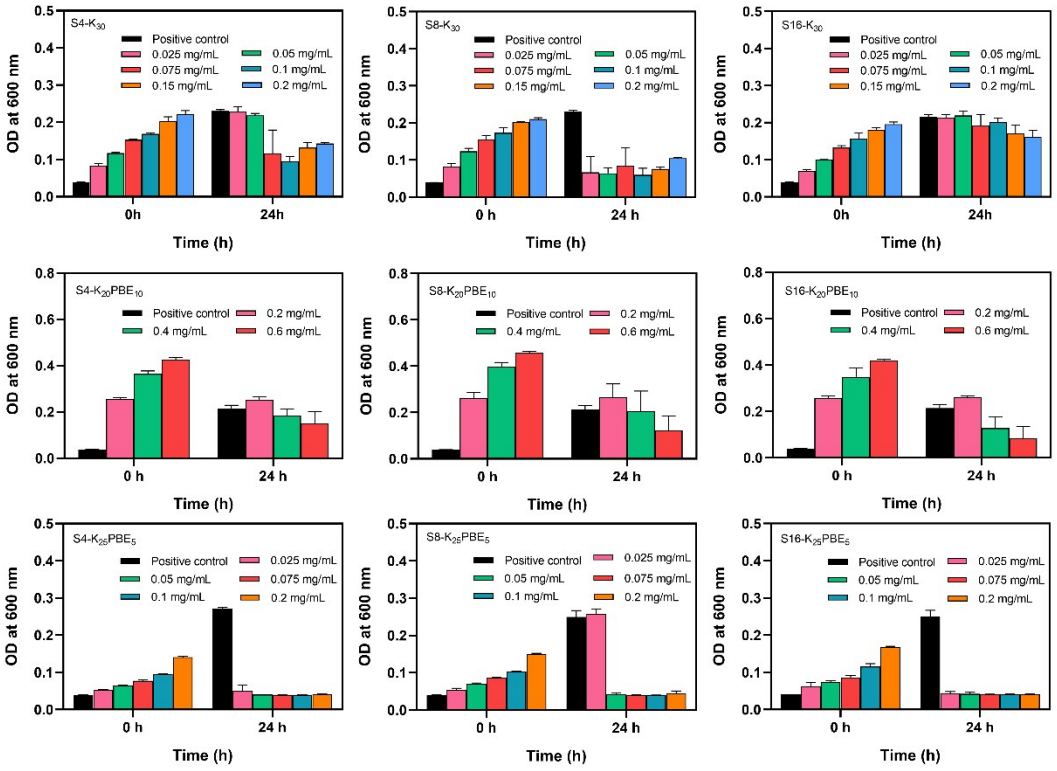

Figure S12. Dose-dependent growth inhibition of *E.coli* in the presence of the resulting polymers.

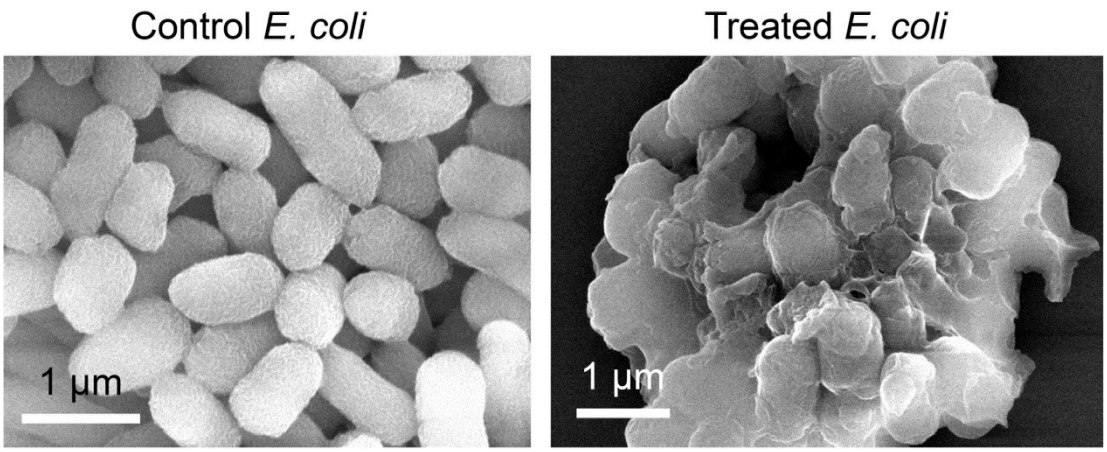

Figure S13. SEM micrographs un- and S4-$K_{25}PBE_5$-OH treated *E. coli* at 4 × MIC for 3 h.

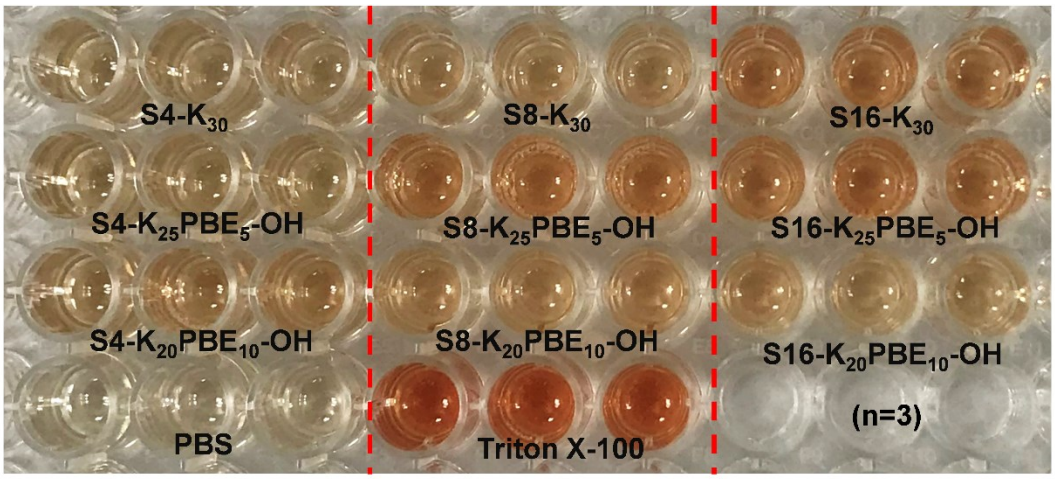

Figure S14. Optical images of the supernatant of mice red blood cells after hemolysis experiment (4 mg·mL^{-1}).

Table S1. The Gx-PAMAM mediated ROP of Boc-$_L$-Lys-NCA

Entry	Sample	Initiator	$[M]_0/[NH_2]_0$	M_n (thero)	M_n (GPC)	M_w/M_n
1	S4-BK_{30}	G0-PAMAM	30	27900	28000	1.15
2	S8-BK_{30}	G1-PAMAM	30	56200	50200	1.07
3	S16-BK_{30}	G2-PAMAM	30	112700	114500	1.05
4	S4-BK_{60}	G0-PAMAM	60	55200	54700	1.03
5	S8-BK_{60}	G1-PAMAM	60	110900	105200	1.01
6	S16-BK_{60}	G2-PAMAM	60	222100	N/A[a]	N/A
7	S4-BK_{100}	G0-PAMAM	100	91700	91500	1.15
8	S4-BK_{200}	G0-PAMAM	200	182900	N/A	N/A
9	S8-BK_{200}	G1-PAMAM	200	366200	N/A	N/A
10	S8-BK_{400}	G1-PAMAM	400	731000	N/A	N/A

[a] The data were not available owing to the bimodal peaks of the GPC curves.